forests

MDPI

Article

Evolutionary Characterization of *tubulin* Gene Family in the Desert Biomass Willow (*Salix psammophila*) and Expression of the *β-tubulin* Gene *SpsTUB10* during Different Stresses

Yujiao He [1], Lijiao Fan [1], Ruiping Wang [2], Shengli Han [3], Guirong Sun [3], Fengqiang Yu [2], Qi Yang [1], Haifeng Yang [1,*] and Guosheng Zhang [1,*]

[1] College of Forestry, Inner Mongolia Agricultural University, Hohhot 010018, China; heyujiao@emails.imau.edu.cn (Y.H.); fanlijiao@emails.imau.edu.cn (L.F.); atp_yangqi@imau.edu.cn (Q.Y.)
[2] Ordos Forestry and Grassland Bureau, Ordos 017010, China; wangnruiping@163.com (R.W.); yufengqiang2024@163.com (F.Y.)
[3] Ordos Afforestation General Farm, Ordos 014300, China; hanshengli2014@163.com (S.H.); sunguirong159@163.com (G.S.)
* Correspondence: haifeng@imau.edu.cn (H.Y.); zgs1960@imau.edu.cn (G.Z.); Tel.: +86-137-0478-6439 (G.Z.)

Abstract: Microtubules, polymerized from α-tubulin (TUA) and β-tubulin (TUB) monomers, play a pivotal role in shaping plant morphogenesis according to developmental and environmental cues. *Salix psammophila* C. Wang & C. Y. Yang is an important shrub plant in sand-fixing afforestation in arid regions, with three significantly distinct plant types shaped under various environments, namely, upright, intermediate, and scattered types. However, how *tubulin* genes respond to the developmental and environmental signs in *S. psammophila* has been far less studied. Here, based on RNA-seq, Sanger sequencing, and real-time PCR (RT-PCR) data, we analyzed the phylogeny of *tubulins* and their expression profiles in *S. psammophila* among the three plant types. Furthermore, we analyzed the genetic structure and expression pattern of *SpsTUB10* in *S. psammophila* under various abiotic stress treatments. In total, we identified 26 *SpsTubulin* genes in *S. psammophila*. The homologous alignment and phylogenetic analysis revealed that these *SpsTubulin* genes can be classified into two groups, corresponding to the *TUA* and *TUB* genes. The expression profiles of these *SpsTubulin* genes in various organs showed that most *SpsTubulin* genes were mainly expressed in the root. *SpsTUB10* is a member of the TUB IIa group, consisting of two intros and three exons. The SpsTUB10 protein contains a typical GTPase domain and a C-terminal domain, with α-helix and random coil dominant in the secondary and tertiary structures. The RT-PCR results of *SpsTUB10* showed an extremely significant difference in expression levels among the root and stem-developing organs between the upright and scattered types, and the transcript level of *SpsTUB10* had a significantly negative correlation with the crown-height ratio. Under different treatments, we found that cold, osmotic stress, and short daylight could significantly increase *SpsTUB10* expression levels compared to those in the controls, thereby supporting the positive role of *SpsTUB10* in stress-induced responses. These results will provide evidence for the *SpsTubulin* genes' response to the developmental and environmental cues in *S. psammophila*.

Keywords: *Salix psammophila*; *tubulin*; *SpsTUB10*; evolutionary analysis; expression analysis; abiotic stress

Citation: He, Y.; Fan, L.; Wang, R.; Han, S.; Sun, G.; Yu, F.; Yang, Q.; Yang, H.; Zhang, G. Evolutionary Characterization of *tubulin* Gene Family in the Desert Biomass Willow (*Salix psammophila*) and Expression of the *β-tubulin* Gene *SpsTUB10* during Different Stresses. *Forests* **2024**, *15*, 696. https://doi.org/10.3390/f15040696

Academic Editor: Om P. Rajora

Received: 4 March 2024
Revised: 31 March 2024
Accepted: 6 April 2024
Published: 13 April 2024

1. Introduction

Plant architecture, indicating the formation of organs correlated with plant morphology, for example, the occurrence of leaves, branches, and flowers during plant growth and development, plays an important role in biomass, landscape, and environmental adaption [1]. In plants, arrays of cortical microtubules (MT), polymerized from the α-tubulin (TUA) and β-tubulin (TUB) proteins, are continually reorganizing to respond to

self-developmental and environmental cues [2], and they play a pivotal role in shaping organ morphogenesis by determining the direction of cell elongation, the cell division plane, and the cellulose deposition [3]. Although multiple TUA and TUB proteins are encoded across kingdoms, the amino acid sequences of these isoforms are typically well conserved, with similarity of the amino acid sequences reaching 88% [4]. This significant conservation in sequences is rooted in constraints imposed by the constitution of the tertiary structure of heterodimers of the tubulins. Electron crystallography approaches reveal that TUA and TUB monomers show nearly identical structures, which can be divided into three domains [5]. The N-terminal domain comprises five α-helices and six parallel β-sheets, with a classical Rossman fold formed and the GTP-binding domain created. The intermediate domain again consists of α-helices and β-sheets, with the binding site for the MT-stabilizing drug taxol formed in β-tubulin. The remaining C-terminal domain contains two α-helices, with a crest formed on the outside surface of the MT protofilament. Copolymerization of TUA and TUB monomers, either in vitro [6] or in vivo [7], has supported the conservation in function of tubulins across organisms. Considering that extreme divergence restricted to the C-terminal domain represents the major source of these isotypic variants, it is thus often proposed that the functional specificity of *tubulin* isoforms is determined by this domain. In addition, post-translational modifications have also generated a variety of *tubulin* isotypes [8].

In plants, a relatively large suite of the *TUA* and *TUB* genes has been extensively reported; for instance, six *TUA* genes encoding nine proteins and at least nine *TUB* genes encoding nine proteins are found in *Arabidopsis thaliana* (L.) Heynh. [9]. In the wood perennial *Populus trichocarpa* Torr. & Gray, 8 *TUA* genes and 20 *TUB* genes are identified [10]. A total of 28 *tubulin* genes are observed in *Salix arbutifolia* Pall. [11] and *Salix purpurea* L. [12]. Genome-wide analysis revealed 23 *tubulin* genes in cassava, with 4 major groups classified based on the types and phylogenetic characteristics [13]. Spatiotemporal expression of *tubulin* genes has been documented in various plants. For example, in *A. thaliana*, the *AtTUA1* gene is only abundant in flowers, but the *AtTUA2*–*AtTUA5* genes are expressed in roots, leaves, and flowers [9]. The transcript of *AtTUB1* is primarily detected in the roots, while the *AtTUB5* and *AtTUB6* transcripts are preferentially expressed in leaves and petioles [14]. The *Populus PtTUA1* and *PtTUA5* are transcribed in wood-forming tissues and pollens, whereas *PtTUA6* and *PtTUA8* are only expressed in pollens [15]. Real-time PCR (RT-PCR) results revealed that the small number of *TUA* families relative to that of *TUB* genes is complemented by a higher number of the copy of each *TUA* transcript [11]. The expression profiles of the cassava *MeTubulins* in various organs showed that the *MeTubulins* are mainly transcribed in the stem, leaf, and petiole [13].

The transcript levels of most *tubulin* genes in plants can be regulated environmentally. The environmental signals are involved in various abiotic stresses, such as temperature (low or high temperature), light, drought, and salinity. Low-temperature-induced (4 °C) alterations in *tubulin* gene expression have been reported in several plants. For example, the expression patterns of both *TUA* and *TUB* isoforms are altered in the leaves of *A. thaliana* during low-temperature exposure; however, with a smaller effect presented for the *TUAs* than for the *TUBs*. An investigation of the *TUB* genes' expression showed that during low-temperature treatment, the transcript levels of *TUB2*, *TUB3*, *TUB6*, and *TUB8* decreased, while those of *TUB4*, *TUB5*, and *TUB7* remained unchanged, and the transcript level of *TUB9* increased [16]. The light-induced downregulation of the *TUB1* transcript level has been reported in seedling hypocotyls of both *Arabidopsis* [17] and soybean [18]. The expression profiles of the *TUA* genes under 250 mM salt treatment were downregulated in both wheat and barley [19]. The environment-mediated regulation of *tubulin* genes has been examined in different tissues of barley [20], potato [21], and *P. euphratica* Oliv [22].

S. psammophila C. Wang & C. Y. Yang is an important shrub plant in sand-fixing afforestation in arid regions due to the strong resistance and reproduction in wind-sand and drought environments [23,24]. According to the morphological differences in plant height and ground diameter (here using the crown-height ratio to mark these differences),

three significantly different plant architectures, namely, upright, intermediate, and scattered types (Figure 1A–C), have been individually found in different habitats for this species [25]. These plant type variations could be beneficial to promote adaptation to the various environments [1]. For example, the upright type possesses strong resistance in lodging and drought and is suitable for the habitats with strong wind-sand and less water. The intermediate type refers to the environments with weak wind-sand and sufficient water to ensure the quality and yield of branches. The scattered type generally has a larger crown area and coverage, and corresponding strong resistance in windbreak and sand-soil fixation, and it is thus suitable for the areas with less wind and more water. However, the genetic basis for shaping such morphological architecture according to environmental cues in *S. psammophila* has not been fully explored. Transcriptome analysis showed that the *ATX1* (encoding copper chaperone protein) + *FHY1* (far-red elongated hypocotyl 1) combination had the greatest influence on the formation of three plant types of *S. psammophila* [26]. However, whether the *tubulin* gene family also plays a role in shaping plant types of *S. psammophila* is far less known, as well as their expression profiles under different abiotic stresses. In this study, we investigated the expression profiles and phylogeny of the *SpsTubulin* genes in *S. psammophila* using RNA-seq data and, furthermore, investigated the evolutionary characterization and expression profiles of *SpsTUB10* under different abiotic stress treatments. Our results will provide evidence for the role of *tubulin* genes in response to the developmental and environmental cues.

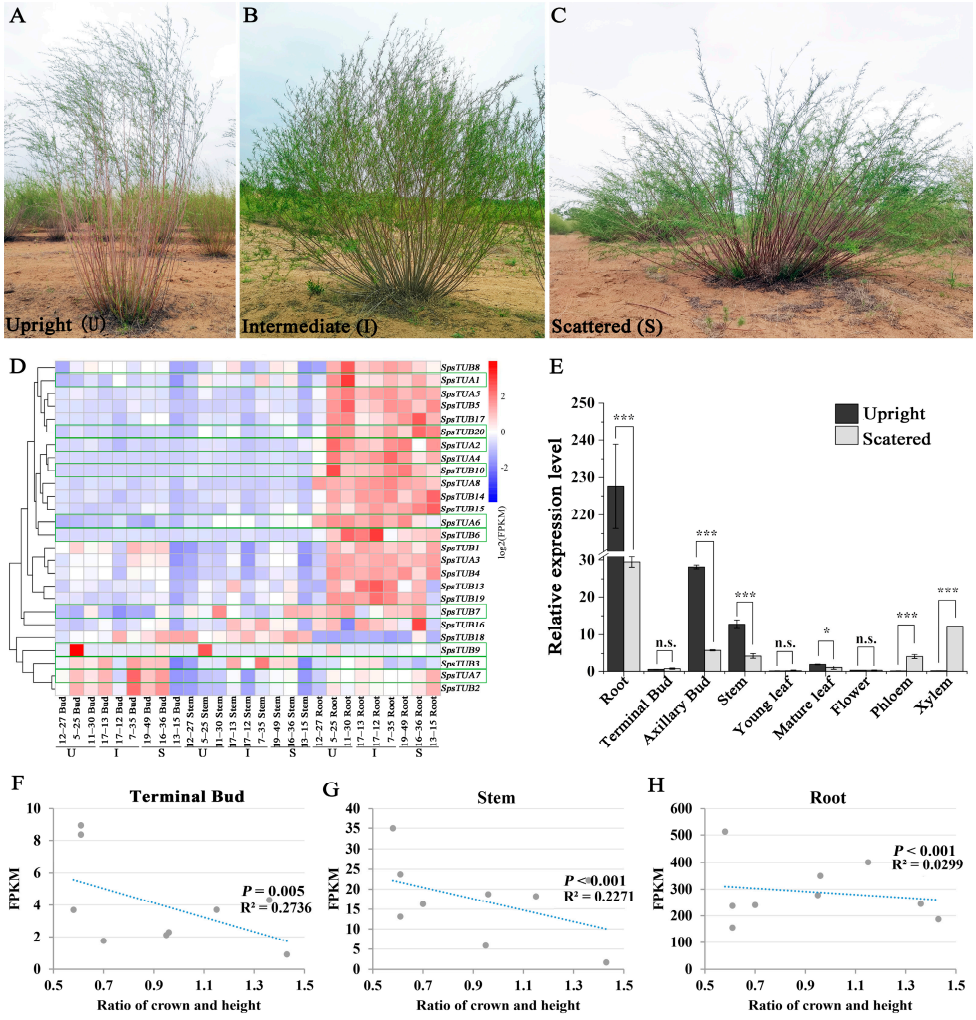

Figure 1. Morphological traits of the three plant types and expression profiles of the *SpsTubulin* genes, and correlation between *SpsTUB10* expression and the crown-height ratio within *Salix psammophiola*.

(**A**–**C**) The upright (U), intermediate (I), and scattered (S) types. (**D**) Expression profiles of the *SpsTubulin* genes based on the RNA-seq data of the three plant types among the root, terminal bud, and stem organs. The organs are classified according to plant types, as marked in (**A**). Among these 26 *SpsTubulin* genes, 10 members (green box for each of them) had relatively longer lengths in CDS sequences, including *SpsTUA1*, *2*, *6*, *7*, and *SpsTUB3*, *6*, *7*, *9*, *10*, and *20*. In particular, *SpsTUB10* showed a significantly higher expression level in the root than those in the bud and stem in comparisons of three plant types, with stable repeats for each organ. *SpsTUB10* was, therefore, used in the downstream analyses. (**E**) Relative expression of *SpsTUB10* among various organs within *S. psammophiola*. (**F**–**H**) The significant line correlation between the expression levels (indicated by FPKM) of *SpsTUB10* and the crown-height ratio within various organs. *** Indicates $p < 0.001$; * indicates $0.01 \leq p < 0.05$; n.s. indicates no significance.

2. Materials and Methods

2.1. Plant Materials

Three-year-old clones of *Salix psammophila*, growing in the National Germplasm Resource Repository of *S. psammophila* in Ordos Dalad Banner, the Inner Mongolia Autonomous Region of China (40.23764° N, 110.64972° E), were used to investigate the plant architecture and the potential role of *SpsTubulin* genes in *S. psammophila*. To distinguish the three plant types, the crown-height ratio was employed by examining the height and ground diameter, with three clone samples for each of the three types [27]. For the crown width, the mean values of the ground diameter from east to west and from south to north were used. Accordingly, the crown-height ratio of the upright type was measured using the clones of 5–25, 11–30, and 12–27, which was less than 0.7. The crown-height ratio of the intermediate type was calculated using the clones of 17–13, 17–12, and 7–35, and it varied between 0.7 and 1.0, while the crown-height ratio of the scattered type was measured using the clones of 19–49, 16–36, and 13–15, and it was more than 1.0 (Table S1).

2.2. Plant Organ Collection and RNA-Sequencing

According to the previous report about the expression patterns of the *TUB* genes within *Salix* [28], many *Salix TUB* genes were not transcribed in different regions of the stem, in conjunction with the expression patterns of *TUB* genes in other species [11,12,16]. We selected the organ samples from the root, terminal bud, and fresh stem (hereafter called stem) for RNA-sequencing (RNA-seq). For these nine clones of the three plant types, different organs from the root, terminal bud, and fresh stem were harvested and stored at −80 °C for total RNA isolation, with three biological replications for each organ sample. Thus, a total of 27 samples were used for RNA-seq (Table S2). An RNA prep Pure Plant Plus Kit (TianGen, Beijing, China) was used to extract total RNA, and a Nanodrop 2000C Bioanalyzer (Thermo, Waltham, MA, USA) was used to assess the quality and quantity of the isolated RNA. The purified RNA for each organ sample was used to prepare cDNA libraries according to the instructions of the TruseqTM RNA Sample Preparation Kit (Illumina, San Diego, CA, USA). The RNA-seq was carried out on an Illumina HiSeq 2500 platform (Novogene, Guangzhou, China) and 200 bp paired-end reads were yielded.

2.3. Identification of the Tubulin Genes Using the RNA-Seq Data

The raw reads were filtered by removing adapter sequences, low-complexity sequences, low-quality bases, with >65% of the bases having a quality score ≤ 7, and the reads with too many (>5%) unknown base calls (N). These clean reads were aligned to the transcripts of *S. purpurea* (https://phytozome.jgi.doe.gov/pz/portal.html#!in%20fo?alias=Org_Spurpurea, accessed on 30 December 2023) using HISAT2 [29]. Next, the transcript levels (FPKM, fragments per kilobase of exon per million fragments mapped [30]) of genes were identified using Stringtie v2.2.0 [31]. The expression level of each gene was obtained by averaging the FPKM values from the three biological replications of each organ. Genes with an average FPKM ≥ 1 were retained for the downstream analyses.

All the newly sequenced transcriptomes of *S. psammophila* in this study were used to identify the TUA and TUB proteins using local BLAST searches based on the protein sequences of 15 *A. thaliana* [9] and 28 *S. purpurea tubulin* genes [12]. The tubulin protein domains were identified using the Hidden Markov Model (HMM) in Pfam (http://pfam.xfam.org, accessed on 3 January 2024). We applied BLASTp to search the amino acid sequences of the tubulin domains against the protein sequences of *S. psammophila*. To remove the redundant sequences, we used SMART (http://smart.embl-heidelberg.de/, accessed on 3 January 2024) to identify the conservative tubulin domains among these putative *tubulin* genes of *S. psammophila*. Multiple alignments of the amino acid sequences of *tubulin* genes were conducted using online ESPript 3.0 (https://espript.ibcp.fr/ESPript/ESPript/index.php, accessed on 3 January 2024).

2.4. Expression Profiles of the SpsTubulin Genes and the Phylogenetic Analysis

To investigate the expression profiles of the *tubulin* gene family between contrast groups of *S. psammophila*, the ratios of the absolute FPKM values divided by the average of all values were transformed by log2 to generate data for clustering displays, and the heatmap was produced by the Hiplot tool (https://hiplot.com.cn/basic/heatmap, accessed on 4 January 2024).

To validate the expression profiles of the *SpsTubulin* genes assessed using RNA-seq data, real-time PCR (RT-PCR) was performed. Among the 26 *SpsTubulin* genes in *S. psammophila*, 10 members (see the results in Figures 1D and 2, with a green box for each of them) have the full lengths in the CDS sequences compared with their homologous genes, including *SpsTUA1*, *2*, *6*, *7*, and *SpsTUB3*, *6*, *7*, *9*, *10*, and *20* (Figure S1). Selecting from these ten *SpsTubulin* genes will ensure the consistency between those assembled using RNA-seq and those cloned via PCR and Sanger sequencing. A previous study showed that the expression pattern diversity of *Salix β-tubulin* gene families might be of important significance in response to the development and environmental demands of perennial woody plants [28]. Considering the significantly higher expression level of *SpsTUB10* in the root than those in the bud and stem in comparisons of the three plant types, and the stable expression levels in each replication of each organ (see the result in Figure 1D), we examined the relative expression levels of *SpsTUB10* using RT-PCR among different organs between the upright and scattered types, which presented a significantly significant difference in the crown-height ratio. To further examine the organ-specific expression pattern of *SpsTUB10*, beyond the root, terminal bud, and stem, we further isolated the total RNA from the axillary bud, young leaves, mature (fully expanded) leaves, flower, stem-developing phloem, and xylem, as described above. All plants were harvested from the National Germplasm Resource Repository of *S. psammophila* clones in Dalad Banner, Inner Mongolia. Real-time PCRs (RT-PCRs) were performed using the TB Green® Premix Ex TaqTM Π (TliRNaseH Plus, Takara, Osaka, Japan) and StepOnePlusTM System (Applied Biosystems, LightCycler® 480 II, Roche, Basel, Switzerland) under a 20 μL volume reaction system, which contained 10.0 μL of 2× TB Green® Premix Ex TaqTM Π Master Mix, 1.0 μL of q-SpsTUB10-F (10 μM), 1.0 μL of q-SpsTUB10-R (10 μM), 1.0 μL of template cDNA, and 7.0 μL of ddH^2O. Pairwise primers (q-SpsTUB10-F and q-SpsTUB10-R; Table S5) were designed as described above. The RT-PCR was performed under the following conditions: 95 °C for 5 min, 40 cycles of 95 °C for 15 s, and 58 °C for 30 s, and then melting (95 °C for 15 s, 60 °C for 1 min, and 95 °C for 15 s) and cooling (40 °C for 5 min). The PCR products were sequenced to ensure amplification specificity based on the dissociation curve. The relative expression level of *SpsTUB10* in each organ was normalized by the expression level of the internal reference *UBQ* gene (glycine soja ubiquitin, GenBank number: SapurV1A.0014s0290.1) and quantified by the $2^{-\Delta\Delta ct}$ method [32]. Each RT-PCR amplification was repeated three independent times, with the transcript levels of the *SpsTUB10* showing no significant change (p-value ≥ 0.95) against the mean value calculated from the three replications. The correlation between the transcript level (FPKM) of *SpsTUB10* and the

crown-height ratio within each of the three plant types was processed using IBM SPSS 27. The significance was tested using a two-tailed, paired Student's *t* test.

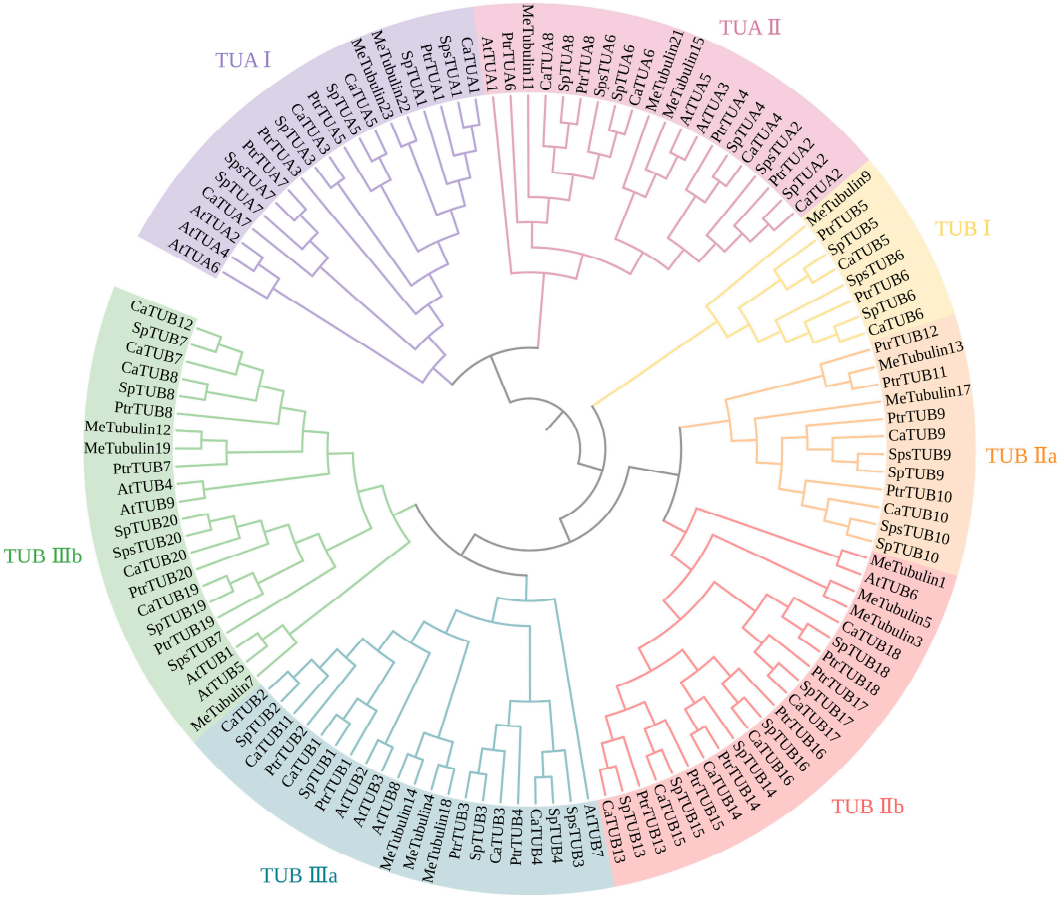

Figure 2. Phylogenetic analysis based on amino acid sequences of the *tubulin* genes among different species. Species short forms: *S. psammophila* (Sps); *S. purpurea* (Sp); *S.* (*Chosenia*) *arbutifolia* (Ca); *P. trichocarpa* (Ptr); *A. thaliana* (At); *M. esculenta* (Me).

The whole tubulin protein sequences for *S. psammophila* (Sps), *S. purpurea* (Sp), *S.* (revised from *Chosenia*) *arbutifolia* (Ca), *Populus trichocarpa* (Ptr), *Arabidopsis thaliana* (At), and *Manihot esculenta* (Me) were retrieved from NCBI (https://www.ncbi.nlm.nih.gov/, accessed on 5 January 2024) and Phytozome 13 (https://phytozome.jgi.doe.gov/pz/portal.html, accessed on 5 January 2024). The accession numbers of these tubulin protein sequences are listed in Table S3. All tubulin proteins were aligned using MEGA 6.0 [32] and checked by the researchers. A neighbor-joining (NJ) phylogenetic tree based on the tubulin protein sequences was reconstructed using MEGA 6.0, with 1000 bootstrap replications. The resulting tree was visualized and beautified on iTOL (https://itol.embl.de/, accessed on 6 January 2024).

2.5. Sequence Analysis and Structural Characterization of SpsTUB10

Among the identified *tubulin* genes of *S. psammophila*, we further conducted analyses on the sequences and structure characteristics of *SpsTUB10*. To clone the full-length sequence of *SpsTUB10*, total genomic DNA (gDNA) was extracted using DP305 (TianGen, Beijing, China) according to the manufacturer's protocol. To clone the CDS of *SpsTUB10*, total RNA was extracted using RNAsimple DP419 (TianGen, Beijing, China) following the instruction manual, and treated with RNase-free Dnase RT411 (TianGen, Beijing, China) to remove contaminating DNA. The first-strand cDNA synthesis and purification were successively conducted using Quant CDNA KR103 (TianGen, Beijing, China) and the E.Z.N.A.®

Gel Extraction Kit (Omega, OmegaBioTek, Norcross, GA, USA), following the corresponding product manuals. Pairwise primers for cloning the *SpsTUB* gene (SpsTUB10-F and SpsTUB10-R; Table S5) were designed using Primer Premier 5.0 according to the CDS sequences of the TUA and TUB genes, which were identified by analyzing the transcriptomes of *S. psammophila*. PCR amplifications were performed in a 20 µL volume containing 1 µL of cDNA, 10 µL of MIX-Taq (TsingKe, Beijing, China), 0.8 µL of SpsTUB10-F (10 µM), 0.8 µL of SpsTUB10-R (10 µM), and 7.6 µL of ddH_2O. The PCR amplifications program was run as follows: 94 °C for 5 min, followed by 38 cycles of 94 °C for 30 s, 61 °C for 45 s, and 72 °C for 2 min. The PCR products were detected using 1% agarose gel in NA-Gel™ E6090 Electrophoresis (Beyotime biotechnology, Shanghai, China). The purified PCR products were sequenced using Sanger sequencing in Qsingke Biotechnology (Xi'an, China) based on the specific primers of *SpsTUB10* (Table S5).

The structure of the exons/introns was determined by comparing genomic DNA and CDS sequences of the *SpsTUB10*. The sequence length and subcellular location prediction of the tubulin proteins of *S. psammophila* were generated using online ExPASy (http://web.expasy.org/protparam/, accessed on 6 January 2024) and the Psort server (https://www.genscript.com/psort.html, accessed on 6 January 2024) by setting the default parameters. The open reading frame of *SpsTUB10* was analyzed using the ORF Finder on NCBI (https://www.ncbi.nlm.nih.gov/orffinder/, accessed on 6 January 2024). The physicochemical properties of *SpsTUB10* were estimated using ExPASy (http://web.expasy.org/protscale/, accessed on 6 January 2024). The signal peptide of *SpsTUB10* was predicted using SingalP 6.0 (https://services.healthtech.dtu.dk/services/SignalP-6.0/, accessed on 6 January 2024). The transmembrane structure of the protein was predicted using the TMHMM Server v. 2.0 (http://dtu.biolib.com/DeepTMHMM, accessed on 6 January 2024). The online MEME program (http://meme.nbcr.net/meme/intro.html, accessed on 6 January 2024) was used to analyze the conservative motifs in the full-length *SpsTUB10* proteins, with the following parameters: the site distribution, any number of repetitions, the number of motifs, the optimum motif length of 10–20 residues, and shuffling the sequences several times under the same parameters to ensure the reliability of the motif. The secondary structure of *SpsTUB10* was predicted by SOPMA on IBCP (https://npsa-prabi.ibcp.fr/, accessed on 6 January 2024), and the tertiary structure was constructed using the SWISS-MODEL in online ExPASy (http://web.expasy.org/protparam/, accessed on 6 January 2024). The amino acid sequences of *TUB* genes of *S. purpurea SpTUB* (Sapur.003G091100.1), *S. arbutifolia CaTUB* (AGH08228.1), *Salix brachista SbrTUB* (KAB5564499.1), *Salix dunnii SdTUB* (KAF9685822.1), *P. trichocarpa PtrTUB* (Potri.003G126800.1), *Populus alba PaTUB* (XP_034887959.1), *Populus tomentosa PtoTUB* (KAG6781065.1), *Populus euphratica PeTUB* (XP_011022700.1), *A. thaliana AtTUB6* (NP_196786.1), *Camellia sinensis CsTUB* (XP_028064909.19), *Camellia lanceoleosa ClTUB* (KAI7993485.1), *M. esculenta MeTub17* (Manes.01G061400.1), *Zea mays ZmTUB1*(NP_001335008.1), *Oryza sativa OsTUB* (LOC_Os03g01530.1), *Solanum lycopersicum SlTUB* (Solyc10g085020.2.1), and *Sorghum bicolor SbiTUB* (Sobic.001G540900.1) were retrieved from NCBI (https://www.ncbi.nlm.nih.gov, accessed on 7 January 2024) and Phytozome 13 (https://phytozome.jgi.doe.gov/pz/portal.html, accessed on 7 January 2024). Amino acid multiple sequence alignment was conducted using T-COFFEE (http://tcoffee.crg.cat/, accessed on 7 January 2024).

2.6. Relative Expression Levels of SpsTUB10 under Different Stress Treatments

For different abiotic stress treatments, we harvested fresh branches from one-year-old clones that grow in the National Germplasm Resource Repository of *S. psammophila* in Ordos Dalad Banner, Inner Mongolia, because they are relatively young and weakly lignified, and thus we could easily observe changes in morphology and expression levels across a relatively short period of time. After hydroponically growing for 24 h in a greenhouse (24 °C, 16 h light and 8 h dark, located in Inner Mongolia Agricultural University), these fresh branches were divided into nine groups for stress treatments, with three biological replications for each group. We first examined the initial expression levels of *SpsTUB10*

for each group to ensure no significant differences among various treatments. Next, for cold and heat stresses, the samples were positioned in 4 °C and 40 °C to grow for 96 h, and to simulate osmotic stress and salt stress, the samples were hydroponically treated with 20% PEG 6000 and 250 mM NaCl for 96 h [19,33]. For these four treatments, a control was set, hydroponically treated under 25 °C. We collected leaves for the treatment and control groups at 0, 1, 2, 3, 4, 6, 8, 12, 24, 48, 72, and 96 h. In addition, the remaining five groups were under light-related treatments across 24 h, including all light (24 h light), short daylight (15 h light and 9 h dark), shorter daylight (9 h light and 15 h dark), all dark (24 h dark), and the control (16 h light and 8 h dark). We collected leaves for the treatment and control groups at 24 h. Meanwhile, the leaves under short and shorter daylight were also collected at 0, 4, 8, 12, 16, 20, and 24 h. All collected leaves were immediately placed in liquid nitrogen and stored at −80 °C for total RNA isolation. To investigate the expression pattern of *SpsTUB10* under different abiotic stress treatments, total RNA was extracted, as described above, and then RT-PCRs were performed, according to the above reaction system and program. Each sample was studied under three biological replications. Relative expression levels of *SpsTUB10* were examined using the $2^{-\Delta\Delta ct}$ method. Statistical differences were studied by one-way ANOVA, and then the post hoc tests were performed to test for significance, with $p < 0.001$ indicating extremely significant, $0.001 \leq p < 0.01$ very significant, $0.01 \leq p < 0.05$ significant, and n.s. referring to not significant. The data were analyzed and plotted in figures using IBM SPSS 27 and Origin 2021.

3. Results

3.1. Transcriptome Sequencing and Expression Profiles of SpsTubulin Genes

Using RNA-sequencing, we obtained 1,241,397,928 clean reads (185.2 Gb clean data) from 27 organ samples of the 3 plant types in *Salix psammophila* (Table S4). Through local BLAST search and HMMER analysis, 26 genes with the tubulin domain were recognized and annotated as *SpsTubulin* genes in the transcriptomes of *S. psammophila*. After aligning the SpsTubulin protein sequences with those of *S. arbutifolia* and *Populus trichocarpa*, 26 *SpsTubuline* genes were named: *SpsTUA1–SpsTUA8*, *SpsTUB1–SpsTUB10*, and *SpsTUB13–SpsTUB20* (Figure 1D).

By using the fragments per kilobase of transcript per million mapped fragments (FPKM), the correlation heatmap analysis can divide these 27 transcriptome samples into 3 groups, corresponding to the root, stem, and terminal bud organs (Figure 1D). The expression profiles of *SpsTubulin* genes in various organs of the three plant types were analyzed using RNA-seq data, and most *SpsTubulin* genes were mainly expressed in the root for each of the three plant types (Figure 1D). Several *SpsTubulin* genes were also found to be expressed in the terminal bud, for example, *SpsTUA7*, *SpsTUB2*, and *SpsTUB3* (Figure 1D).

To validate the expression profiles of the *SpsTubulin* genes based on RNA-seq data, we selected *SpsTUB10* to examine the relative transcript level using RT-PCR among different organs between the upright and scattered types (Figure 1E). The results showed an extremely significant difference in the expression levels of *SpsTUB10* in the root and stem-developing organs (including the axillary bud, stem, phloem, and xylem; $p < 0.001$). The expression levels of *SpsTUB10* in the root and stem were consistent with the RNA-seq data, while that in the bud did not agree with the RNA-seq data (Figure 1D,E). In addition, significantly different *SpsTUB10* expression levels were also detected in the mature leaves ($0.01 \leq p < 0.05$; Figure 1E), and no significant difference in *SpsTUB10* expression was detected in the terminal bud, young leaves, and flower ($p > 0.05$; Figure 1E). To ensure the potential role of *SpsTUB10* in the plant types of *S. psammophila*, we performed a correlation analysis between the transcript level of *SpsTUB10* (indicated by FPKM) and the crown-height ratio. A significantly negative correlation between the FPKM and the crown-height ratio was found in the terminal bud, stem, and root, with all $p < 0.01$ (Figure 1F–H).

3.2. Phylogenetic Analysis of the SpsTubulin Genes

Among the 26 identified *SpsTubulin* genes in *S. psammophila*, the CDS sequences of 16 *SpsTubulin* genes were too short (<100 bp) to align with other *tubulin* genes, and thus were removed in the phylogenetic analysis. Based on the tubulin protein sequences of *S. psammophila* (Sps), *S. purpurea* (Sp), *S.* (*Chosenia*) *arbutifolia* (Ca), *Populus trichocarpa* (Ptr), *Arabidopsis thaliana* (At), and *Manihot esculenta* (Me), an unrooted neighbor-joining (NJ) tree was constructed, and their phylogenetic relationships were further analyzed. A total of 129 tubulin protein sequences, including 10 SpsTubulins, 26 SpTubulins, 28 CaTubulins, 28 PtrTubulins, 15 AtTubulins, and 22 MeTubulins, were classified into the two groups corresponding to the TUA and TUB proteins (Figure 2). According to the classification of Rao et al. [11], the TUA group can be further divided into TUA I and TUA II, and the TUB group can be divided into TUB I, TUB Iia, TUB Iib, TUB IIIa, and TUB IIIb (Figure 2). TUA I consisted of SpsTUA1 and SpsTUA7, together with four SpTubulins (SpTUA1, 3, 5, and 7), four CaTubulins (CaTUA1, 3, 5, and 7), four PtrTubulins (PtrTUA1, 3, 5, and 7), three AtTubulins (AtTUA2, 4, and 6), and two MeTubulins (MeTubulin22 and 23) (Figure 2). For TUA II, two SpsTubulins (SpsTUA2 and 6), four SpTubulins (SpTUA2, 4, 6, and 8), four CaTubulins (CaTUA2, 4, 6, and 8), four PtrTubulins (PtrTUA2, 4, 6, and 8), three AtTubulins (AtTUA1, 3, and 5), and three MeTubulins (MeTubulin11, 15, and 21) were clustered (Figure 2). One SpsTubulin (SpsTUB6), two SpTubulins (SpTUB5 and 6), two CaTubulins (CaTUB5 and 6), two PtrTubulins (PtrTUB5 and 6), and one MeTubulin (MeTubulin9) belonged to TUB I (Figure 2). Two SpsTubulin genes (SpsTUB9 and 10), two SpTubulins (SpTUB9 and 10), two CaTubulins (CaTUB9 and 10), four PtrTubulins (PtrTUB9, 10, 11, and 12), and two MeTubulins (MeTubulin13 and 17) mainly fell into TUB Iia (Figure 2). Six SpTubulins (SpTUB13, 14, 15, 16, 17, and 18), six CaTubulins (CaTUB13, 14, 15, 16, 17, and 18), six PtrTubulins (PtrTUB13, 14, 15, 16, 17, and 18), one AtTubulin (AtTUB6), and three MeTubulins (MeTubulin1, 3, and 5) mainly joined TUB Iib (Figure 2). TUB IIIa mainly consisted of one SpsTubulin (SpsTUB3), four SpTubulins (SpTUB1, 2, 3, and 4), five CaTubulins (CaTUB1, 2, 3, 4, and 11), four PtrTubulins (PtrTUB1, 2, 3, and 4), four AtTubulins (AtTUB2, 3, 7, and 8), and three MeTubulins (MeTubulin4, 8, and 14) (Figure 2). Similarly, TUB IIIb, including three introns, mainly consisted of two SpsTubulin genes (SpsTUB7 and 20), four SpTubulins (SpTUB7, 8, 19, and 20), five CaTubulins (CaTUB7, 8, 12, 19, and 20), four PtrTubulins (PtrTUB7, 8, 19, and 20), four AtTubulins (AtTUB1, 4, 5, and 9), and three MeTubulins (MeTubulin7, 12, and 19) (Figure 2). Based on these results, we found that 10 SpsTubulin genes in *S. psammophila* can be classified into 6 groups, without tubulin members found in TUB IIb (Figure 2).

3.3. Cloning, Sequence, and Structural Analyses of SpsTUB10

To well document the spatial-temporal expression pattern of the *tubulin* genes within *S. psammophila* under various abiotic stresses, we selected the *SpsTUB10* gene for the following analyses. Phylogenetic analysis showed that the *SpsTUB10* gene belongs to TUB IIa (Figure 2). The PCR bands showed a clear difference between the full-length *SpsTUB10* gene and its CDS, both of which were nearly positioned at 1500 bp and 1300 bp (Figure 3A). The Sanger sequencing showed that the full-length *SpsTUB10* was 1502 bp and its CDS was 1335 bp. This result was consistent with the CDS length (1335 bp) predicted by the NCBI OFR finder. The gene structure predication showed that *SpsTUB10* consisted of two introns and three exons, with the length of intro1 of 90 bp and that of intro2 of 77 bp (Figure 3B). ExPASy ProtParam analysis showed that the *SpsTUB10* gene encoded 443 amino acids (Figure 3B). Among them, glycine (Gly) was the most abundant (8.1%), followed by glutamic acid (Glu, 7.2%; Figure S2). The molecular weight was 49,747.98 Da, the theoretical isoelectric point was 4.85, and the theoretical molecular formula was $C_{2175}H_{3344}N_{596}O_{680}S_{32}$. The predicted subcellular localization showed that 73.9% of SpsTUB10 was localized in the cytoplasm, and the rest was positioned in the nucleus, plasmolemma, peroxide membrane, and mitochondrion. The SpsTUB10 protein contained 58 negatively charged residues (Asp + Glu) and 36 positively charged residues (Arg + Lys), with a half-life of 30 h and an

instability index (33.11) of less than 40, indicating that it is a stable protein. The SpsTUB10 protein was hydrophilic, with a grand average of hydropathicity index (GRAVY) of −0.379, and it had no transmembrane structure or signal peptide region.

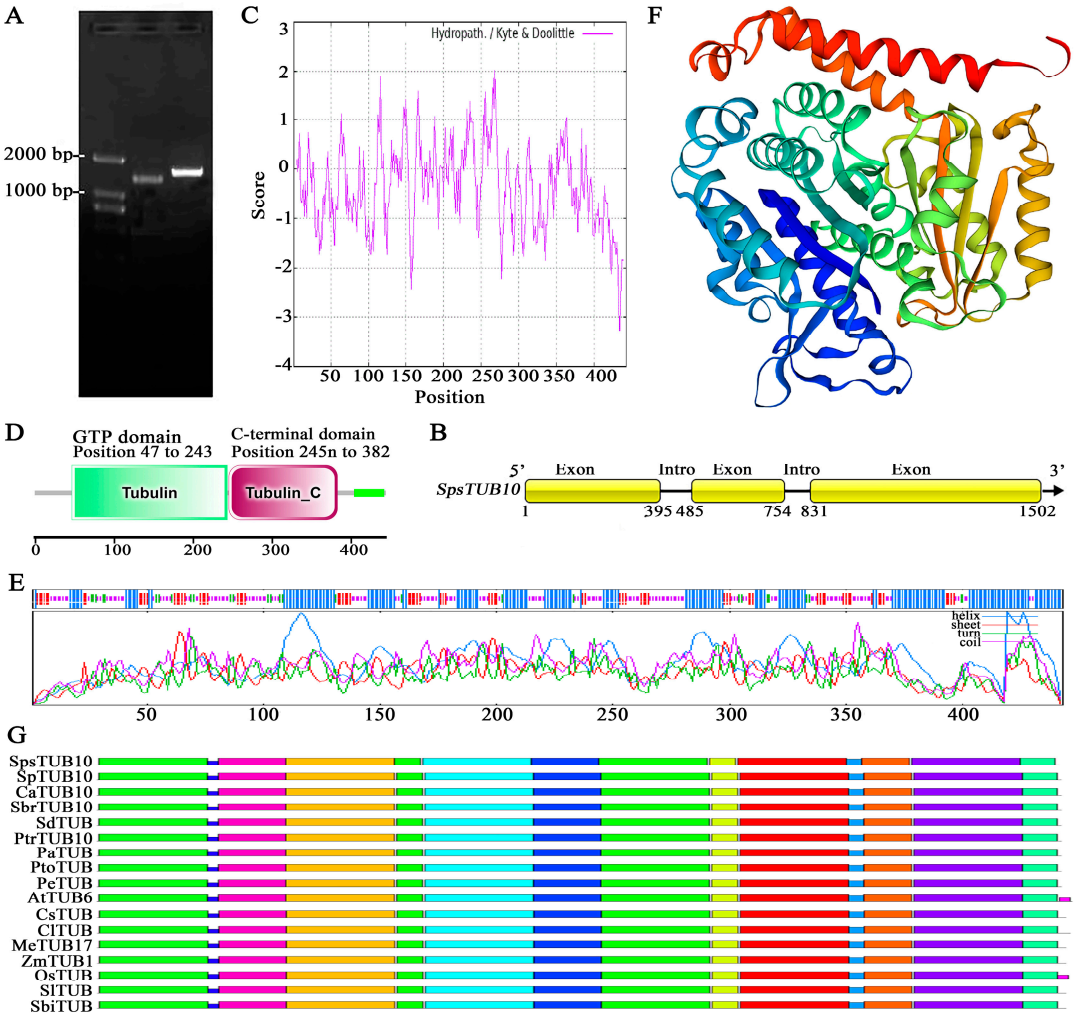

Figure 3. Structure features of the *SpsTUB10* gene in *Salix psammophila*. (**A**) Target bands of the full length of the *SpsTUB10* gene and its CDS. (**B**) Gene structure of the *SpsTUB10* gene. (**C**) Distributing curve of the hydropathy of SpsTUB10 amino acids. (**D**) Conserved structural domain analysis of SpsTUB10. (**E**) Predicated amino acid secondary structure of SpsTUB10. Blue, α-helix; red, extended strand; yellow, random coil; green, β-turn. (**F**) Predicated amino acid tertiary structure of SpsTUB10. (**G**) Homologous structure alignment of the amino acid sequences of TUB genes between SpsTUB10 in *S. psammophila* and those of the other 16 plants. Bar = 0.1 substitutions per site. The accessions retrieved from NCBI and Phytozome 13, including: *S. purpurea* SpTUB, *S. arbutifolia* CaTUB, *S. brachista* SbrTUB, *S. dunnii* SdTUB, *P. trichocarpa* PtrTUB, *P. alba* PaTUB, *P. tomentosa* PtoTUB, *P. euphratica* PeTUB, *A. thaliana* AtTUB6, *C. sinensis* CsTUB, *C. lanceoleosa* ClTUB, *Manihot esculenta* MeTub17, *Zea mays* ZmTUB1, *O. sativa* OsTUB, *Solanum lycopersicum* SlTUB, and *Sorghum bicolor* SbiTUB.

Conservative structural domain predication in online NCBI showed that the SpsTUB10 protein contained a typical GTPase domain (Tubulin/FtsZ family) and a C-terminal domain (Tubulin/FtsZ family; Figure 3D). According to the SOPMA predictions, the secondary structure of the SpsTUB10 protein consisted of 43.34% α-helix (Hh), 16.93% extended strand (Ee), 33.41% random coil (Cc), and 6.32% β-turn (Tt; Figure 3E). The N- and C-terminal domains of the SpsTUB10 protein were composed of Hh (Figure 3E). The SWISS-MODEL tertiary structure predication indicated that the SpsTUB10 protein was dominated by Hh and Cc (Figure 3F), consistent with the predicted secondary structure.

By using T-COFFEE prediction, we compared the amino acid sequences of the SpsTUB10 protein to the other 16 plant TUBs, including *S. psammophila* SpsTUB10, *S. purpurea* SpTUB, *S. arbutifolia* CaTUB, *S. brachista* SbrTUB, *S. dunnii* SdTUB, *P. trichocarpa* PtrTUB, *P. alba* PaTUB, *P. tomentosa* PtoTUB, *P. euphratica* PeTUB, *A. thaliana* AtTUB6, *C. sinensis* CsTUB, *C. lanceoleosa* ClTUB, *M. esculenta* MeTub17, *Zea mays* ZmTUB1, *Oryza sativa* OsTUB, *Solanum lycopersicum* SlTUB, and *Sorghum bicolor* SbiTUB. The results showed that the amino acid sequence similarity was over 94% among these species, with the highest similarity between SpsTUB10 and SpTUB10 (99.55%), followed by PtTUB10 (98.42%) and CsTUB (96.19%; Figures 3G and S3). Overall, 15 conserved motifs were identified in SpsTUB10, and the tubulin members with similar motif compositions grouped together on the phylogenetic tree. The SpsTUB10 protein had six characteristic structural domains, I, II, III, IV, V, and VI, of microtubule proteins, with highly conserved sequences at the N-terminus and 15 amino acid residues at the C-terminus (red line in Figure S4).

3.4. Expression of the SpsTUB10 Gene under Various Abiotic Stresses

To explore the spatial-temporal expression pattern of *SpsTUB10* in *S. psammophila* under different abiotic stress treatments, we examined the relative expression levels of *SpsTUB10* under temperature-related (cold and heat), osmotic stress, salt, and light-related (all light, all dark, short daylight, and shorter daylight) treatments, with control experiments. We found significant changes in morphology under different stress treatments, especially under the heat and salt stresses, with extremely severe leaf wilting (Figure 4A–I). The relative expression levels of *SpsTUB10* under temperature-related stresses showed clearly distinct patterns with not significantly different transcript levels of *SpsTUB10* before cold or heat stress treatments (Figure 4E). For example, under cold (4 °C) stress, the expression level of *SpsTUB10* continuously increased during the first 48 h, and then decreased under cold treatment. This was similar to *SpsTUB10* expression in the control (25 °C), except for at the peak time three hours after treatment. However, a nearly decreasing tendency of *SpsTUB10* expression was found under heat stress (40 °C; Figure 4E). *SpsTUB10* expression under cold stress was significantly higher than that under heat stress at any time points, while *SpsTUB10* expression under the control was significantly higher than that under both cold and heat treatments during the first 6 h (Figure 4E). Under osmotic and salt stress treatments, we found that the *SpsTUB* expression levels were not significantly different before treatments, and then they increased under osmotic stress over time, with significantly higher levels after 12 h than that under salt and control treatments. *SpsTUB10* expression increased within the first 4 h and then decreased under salt treatment (Figure 4F). Under light-related stress treatments, we found that *SpsTUB10* expression was significantly higher under short daylight, followed by all dark and shorter daylight (Figure 4K). No significant difference was found between control and all light treatments (Figure 4K). In addition, we found that *SpsTUB10* expression was significantly higher under shorter daylight than that under short daylight during the first 16 h (all $p < 0.01$), while the *SpsTUB10* expression levels significantly decreased under shorter daylight after 16 h, compared to that under short daylight (Figure 4L).

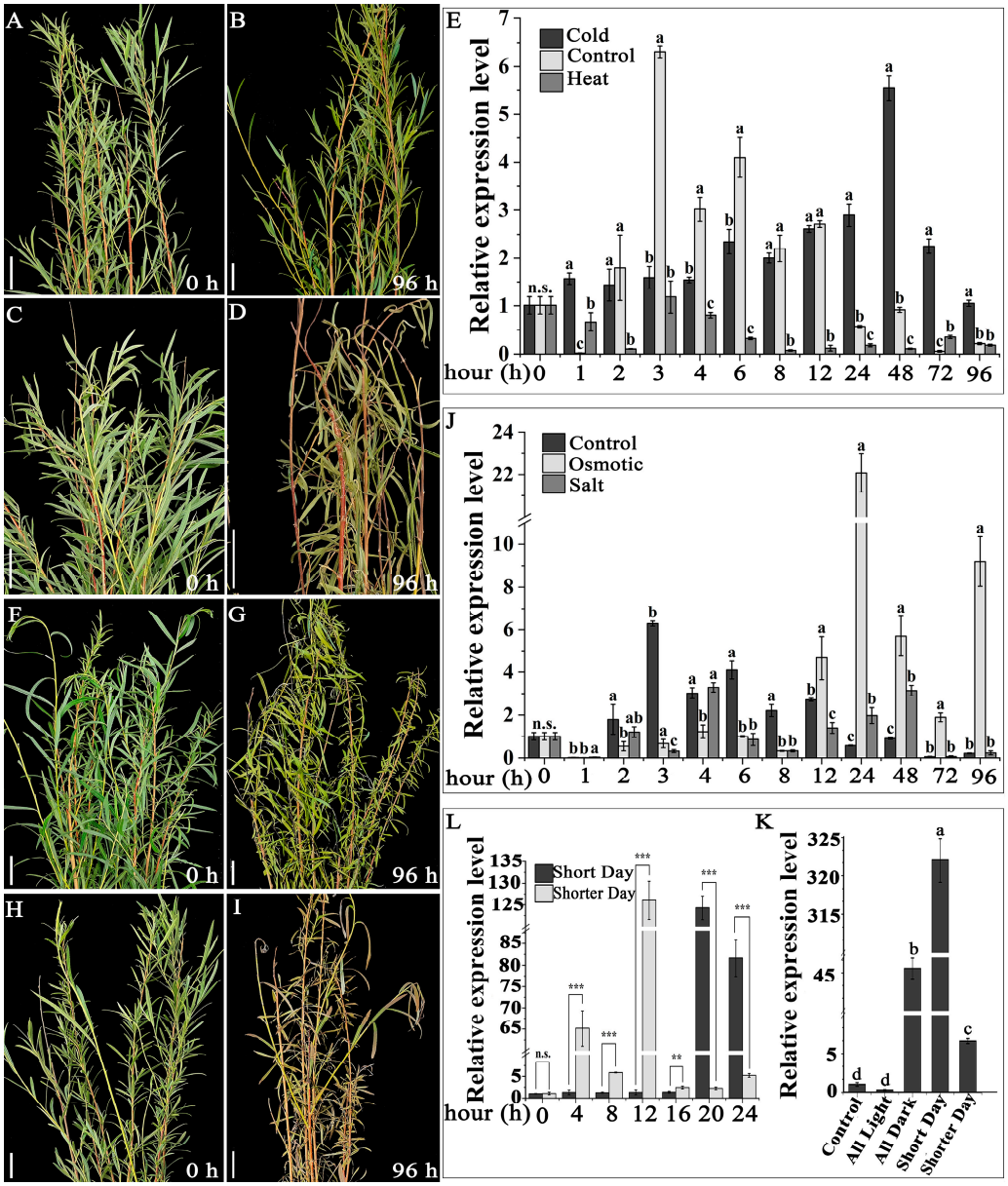

Figure 4. Plant morphological changes and relative expression levels of the *SpsTUB10* gene in *Salix psammophila* during various treatments. (**A**–**D**) Morphological changes under (**A**,**B**) cold (4 °C) and (**C**,**D**) heat (40 °C) treatments from 0 to 96 h. (**E**) Relative expression levels of *SpsTUB10* among cold, control, and heat treatments. (**F**–**I**) Morphological changes under (**F**,**G**) osmotic and (**H**,**I**) salt treatments from 0 to 96 h. (**J**) Relative expression levels of *SpsTUB10* among control, osmotic stress, and salt treatments. (**K**) Relative expression levels of *SpsTUB10* among light-related treatments. (**L**) Relative expression levels of *SpsTUB10* between short and shorter daylight treatments. Significance indicated by $p < 0.05$, with the same lowercase letter in each group representing no significance. *** Indicates $p < 0.001$; ** indicates $0.001 \leq p < 0.01$; n.s. indicates no significance. Scale bar: 3 cm.

4. Discussion

The transcript levels of most *tubulin* genes in plants can be regulated developmentally and environmentally. Understanding the functions of *SpsTubulin* genes in *Salix psammophila* will provide insights for forming different plant types and adapting various environments. In our study, the phylogeny of *SpsTubulin* genes and their expression profiles in *S. psammophila* among the three plant types were analyzed. Furthermore, the genetic structure and expression patterns of *SpsTUB10* in *S. psammophila* under various abiotic stress treatments

were investigated. In this study, 26 *SpsTubulin* genes were identified using the RNA-seq data and named as *SpsTUA1*–*SpsTUA8*, *SpsTUB1*–*SpsTUB10*, and *SpsTUB13*–*SpsTUB20*, according to homologous alignment with tubulin proteins of *S. arbutifolia* and *Populus trichocarpa*. The number of *SpsTubulin* genes was lower than that of other *Salix* and *Populus* species [12], probably due to some *tubulin* genes not being successfully assembled using RNA-seq data. When constructing phylogeny of these *SpsTubulin* genes, 16 members were removed due to their too-short CDS sequences for alignments. The phylogenetic tree showed that the remaining 10 *SpsTubulin* genes can be divided into two main groups, TUA and TUB, and both were further classified into different subgroups. Notably, no *SpsTubulin* genes were screened for the TUB IIb group (Figure 2).

Based on the RNA-seq data, the expression profiles of *SpsTubulin* genes in various organs of the three plant types were analyzed, which could be helpful to study the potential function of the *SpsTubulin* genes (Figure 1). We found that *SpsTubulin* genes were mainly expressed in specific organs, especially in the root, for each of the three plant types (Figure 1). For example, *SpsTUA2* and *SpsTUA6* were highly expressed in the root, which is similar to the homologous genes of *AtTUA1*, *AtTUA3*, and *AtTUA5* [9]. This suggests that *SpsTubulin* expression might play a role in the growth and development of the corresponding organs. The transcript of *SpsTUA7* was mainly found in the terminal bud, and that of *SpsTUA1* was mainly observed in the root, while the homologous genes in cassava, such as *MeTubulin22* and *MeTubulin23*, were mainly expressed in petioles and stems [13], indicating the tissue-specific expression pattern among different species. In addition, in combination with the relatively stable differential expression levels of *SpsTUB10* between the root and the bud/stem, the significantly negative correlation between the *SpsTUB10* expression level (FRPK) and the crown-height ratio might suggest the potential function of *SpsTUB10* in shaping the different plant types in *S. psammophila*. Considering the significantly higher root-specific expression pattern of *SpsTUB10*, a new insight concerning the relationship between the root and plant type formation might have been provided. However, this needs further examination in future studies.

Field investigations showed that abiotic stresses may have played a key role in the growth and development of *S. psammophila*. *SpsTUB10* is a member of the TUB IIb group in the phylogenetic tree (Figure 2). The biological information analysis on the subcellular localization prediction, gene structure, and conservative motifs of *SpsTUB10* supported the evolutionary conservative development. The *SpsTUB10* expression showed a significant difference between the upright and scattered types in the root and the stem-developing organs (Figure 1E), suggesting a regulatory function in the growth and development of *S. psammophila*. The significantly negative correlation between the transcript level of *SpsTUB10* and the crown-height ratio (Figure 1F–H) also likely provides evidence for the regulatory role in shaping the different plant types in *S. psammophila*. Therefore, *SpsTUB10* was further selected for different abiotic stress treatments, and its potential functions were further studied by examining the transcript levels under different treatments. Temperature-related stress (low or high temperature) has significant limitations on the plant growth and development, thereby substantially controlling the crop yield and the geographic distribution pattern of many plants [34]. Plants have evolved diverse mechanisms to respond to temperature-related stress, including cytoskeletal rearrangement and membrane modifications, both for cold [35] and heat stresses [36]. Regarding drought stress (too little water), it will primarily cause hyperosmotic stress for plant cells [37]. In contrast, salt stress (too much salt) has both ionic/ion toxicity and osmotic effects on plant cells [37]. It has been illustrated that the ABA signaling pathway is central in plants' responses to both drought and salt stresses [38]. In addition, the ABA signing pathway also has a role in cold-induced responses [39]. Light not only plays a role in regulating plant growth and productivity, but it is also crucial in determining the accumulate–assimilation and photosynthetic rate. However, the excessive or inadequate exposure of light intensities will negatively affect the plants by inhibiting the physiological metabolic processes [40]. Our RT-PCR results revealed a significant increase in the levels of *SpSTUB10* transcripts under

cold and osmotic stress after 12 h, but always low levels of *SpsTUB10* transcripts under heat and salt treatments (Figure 4E,J), supporting a positive role of *SpsTUB10* in response to cold and osmotic stresses in *S. psammophila*, but not under heat and salt stresses. It is noteworthy that the *SpsTUB10* expression pattern under cold and osmotic stresses showed a gradual tolerance of *S. psammophila* to cold and osmotic stress. This is probably because although the cold temperature (0–15 °C) used herein for low-temperature treatment was low, it coincides with the tolerance level of *S. psammophila* [41]. A highly similar reason is also suggested under osmotic treatment. These hypotheses are also supported by the strong tolerance of *S. psammophila* to cold and osmotic stress. Correspondingly, high-temperature (40 °C) and high-salt (250 mM) treatments could have seriously affected the plant growth via the injury in protein denaturation and ionic/ion toxicity and osmotic effects on plants and, thus, low transcript levels of *SpsTUB10* were identified. Interestingly, the level of the *SpsTUB* transcripts was significantly higher under excessive or inadequate (compared to the control experiment) light treatments, except under all light (Figure 4L), probably supporting that such a high light stress could have exacerbated ROS production and then overwhelmed ROS-managing systems [34]. It is noteworthy that the expression levels of *SpsTUB10* under short and shorter daylight presented an ebb and flow pattern (Figure 4K), indicating strong tolerance of *S. psammophila* to light stress. From these results, the main environmental stresses to *S. psammophila* may be heat and salt. This mainly determines *S. psammophila* growth in sand and arid soils. In addition, the significant changes in *SpsTUB10* expression under different stresses may provide evidence of shaping various plant types to adapt to diverse environments. However, the function of *SpsTUB10* in *S. psammophila* in response to developmental and environmental cues needs further study. Furthermore, the similar cold and osmotic stress-induced responses of *SpsTUB10* will provide a system to examine the interaction mechanism between cold and osmotic stresses, as well as that between different light intensities. Based on these results, we concluded that the *SpsTUB10* gene might have a role in *S. psammophila* in response to the developmental and environmental cues.

5. Conclusions

In this study, an RNA-seq-based *tubulin* gene family analysis in *Salix psammophila* was carried out, and 10 *SpsTubulin* genes were identified. The expression profiles of these *SpsTubulin* genes provide evidence for their potential roles in specific organs among the three plant types. *SpsTUB10*, a member of the TUB IIa group, had a significantly different expression between the root and terminal bud/stem, and it was significantly negative correlated with the crown-height ratio of plant types. The biological information analysis on SpsTUB10 provided the biochemical characteristics of subcellular localization prediction, conservative motifs, and gene structure. Furthermore, the *SpsTUB10* gene expression under various treatments showed a comprehensive response to temperature-related stresses (cold and heat), osmotic, salt, and light-related stresses (all light, all dark, short daylight, and shorter daylight). In summary, these results laid a foundation for further studying the function of the *SpsTubulin* genes.

Supplementary Materials: The following supporting information can be downloaded at: https://www.mdpi.com/article/10.3390/f15040696/s1, Table S1: The characteristic summary of three plant types within *Salix psammophila*. Table S2: Organs used for transcriptome sequencing for different plant types within *Salix psammophila*. Bud indicates the terminal bud. Table S3: Accession number of the *tubulin* genes used for phylogenetic analysis. Table S4: Detailed information on the sequenced transcriptomes for different organs from the clones of the three plant types. Table S5: Information on primers used in this study. Figure S1: Alignment of the amino acid sequences of the *tubulin* genes within *Salix psammophila*. Figure S2: Full length of the cDNA of *SpsTUB10* and its amino acid sequence. Figure S3: Homologous structure alignment of the amino acid sequences of *TUB* genes. Figure S4: Amino acid sequence alignment of SpsTUB10 with 16 other TUB homologous genes from different plant species.

Author Contributions: Conceptualization, Y.H. and G.Z.; methodology, Y.H., L.F. and Q.Y.; software, Y.H. and L.F.; validation, L.F. and Q.Y.; formal analysis, Y.H.; investigation, G.S., R.W., F.Y. and S.H.; resources, G.S., R.W., F.Y. and S.H.; data curation, G.S., R.W., F.Y. and S.H.; writing—original draft preparation, Y.H.; writing—review and editing, Y.H.; visualization, L.F. and Q.Y.; supervision, G.Z. and H.Y.; project administration, G.Z. and H.Y.; funding acquisition, G.Z. and H.Y. All authors have read and agreed to the published version of the manuscript.

Funding: This research was funded by the Inner Mongolia Autonomous Region Applied Technology Research and Development Fund Project (2021GG0075), the Inner Mongolia Autonomous Region Science and Technology Plan Project (2023YFHH0106), the Inner Mongolia Autonomous Region Natural Science Gene Project (2023MS03050), and the Task Book for Key R&D Plan Projects in Ordos City (YF20232319).

Data Availability Statement: Data are contained within the article and Spplementary Materials.

Acknowledgments: We would like to express our gratitude to the Gene Bank of Germplasm Resources of *Salix psammophila* in Ordos Dalad, the Inner Mongolia Autonomous Region of China, and to all those who have contributed to this article.

Conflicts of Interest: The authors declare that they have no conflicts of interest.

References

1. Barthélémy, D.; Caraglio, Y. Plant architecture: A dynamic, multilevel and comprehensive approach to plant form, structure and ontogeny. *Ann. Bot.* **2007**, *99*, 375–407. [CrossRef] [PubMed]
2. Wasteneys, G.O. Progress in understanding the role of microtubules in plant cells. *Curr. Opin. Plant Biol.* **2004**, *7*, 651–660. [CrossRef] [PubMed]
3. Ledbetter, M.C.; Porter, K.R. A "microtubule" in plant cell fine structure. *J. Cell Biol.* **1963**, *19*, 239–250. [CrossRef] [PubMed]
4. Dutcher, S.K. The tubulin fraternity: Alpha to eta. *Curr. Opin. Cell Biol.* **2001**, *13*, 49–54. [CrossRef] [PubMed]
5. Nogales, E.; Wolf, S.G.; Downing, K.H. Structure of the αβ tubulin dimer by electron crystallography. *Nature* **1998**, *391*, 199–203. [CrossRef] [PubMed]
6. Bondstar, J.F.; Fridovich-Keil, J.L.; Pillus, L.; Mulligan, R.C.; Solomon, F. A chicken-yeast chimeric β-tubulin protein is incorporated into mouse microtubules in vivo. *Cell* **1986**, *44*, 461–468.
7. Anthony, R.G.; Hussey, P.J. Dinitroaniline herbicide resistance and the microtubule cytoskeleton. *Trends Plant Sci.* **1999**, *4*, 112–116. [CrossRef]
8. Onelli, E.; Idilli, A.I.; Moscatelli, A. Emerging roles for microtubules in angiosperm pollen tube growth highlight new research cues. *Front. Plant Sci.* **2015**, *6*, 51. [CrossRef]
9. Paredez, A.; Somerville, C.; Ehrhardt, D. Visualization of cellulose synthase demonstrates functional association with microtubules. *Science* **2006**, *312*, 1491–1495. [CrossRef]
10. Chen, X.; Grandont, L.; Li, H.; Hauschild, R.; Paque, S.; Abuzeineh, A.; Ralcusova, H.; Benkova, E.; Perrot-Rechenmann, C.; Friml, J. Inhibition of cell expansion by rapid ABP1-mediated auxin effect on microtubules. *Nature* **2014**, *516*, 90–93. [CrossRef]
11. Rao, G.; Zeng, Y.; He, C.; Zhang, J. Characterization and putative post-translational regulation of α- and β-*tubulin* gene families in *Salix arbutifolia*. *Sci. Rep.* **2016**, *6*, 19258. [CrossRef] [PubMed]
12. Zhou, R.; Macaya-Sanz, D.; Carlson, C.H.; Schmutz, J.; Jenkins, J.W.; Kudrna, D.; Sharma, A.; Sandor, L.; Shu, S.; Barry, K.; et al. A willow sex chromosome reveals convergent evolution of complex palindromic repeats. *Genome Biol.* **2020**, *21*, 38. [CrossRef] [PubMed]
13. Li, S.; Cao, P.; Wang, C.; Guo, J.; Zang, Y.; Wu, K.; Ran, F.; Liu, L.; Wang, D.; Min, Y. Genome-wide analysis of *tubulin* gene family in cassava and expression of family member *FtsZ2-1* during various stress. *Plants* **2021**, *10*, 668. [CrossRef] [PubMed]
14. Li, S.; Lei, L.; Somerville, C.; Gu, Y. Cellulose synthase interactive protein 1 (CSI1) links microtubules and cellulose synthase complexes. *Proc. Natl. Acad. Sci. USA* **2012**, *109*, 185–190. [CrossRef] [PubMed]
15. Oakley, R.V.; Wang, Y.S.; Ramakrishna, W.; Harding, S.A.; Tsai, C.J. Differential expansion and expression of α- and β-*tubulin* gene families in *Populus*. *Plant Physiol.* **2007**, *145*, 961–973. [CrossRef] [PubMed]
16. Chu, B.; Snustad, D.P.; Carter, J.V. Alteration of *β-tubulin* gene expression during low-temperature exposure in leaves of *Arabidopsis thaliana*. *Plant Physiol.* **1993**, *103*, 371–377. [CrossRef] [PubMed]
17. Leu, W.M.; Cao, X.L.; Wilson, T.J.; Snustad, D.P.; Chua, N.H. Phytochrome A and phytochrome B mediate the hypocotyl-specific downregulation of *TUB1* by light in *Arabidopsis*. *Plant Cell* **1995**, *7*, 2187–2196.
18. Jongewaard, I.; Colon, A.; Fosket, D.E. Distribution of transcripts of the *tubB1* gene in developing soybean (*Glycine max* [L.] Merr.) seedling organs. *Protoplasma* **1994**, *18*, 77–85. [CrossRef]
19. Temel, A.; Gozukirmizi, N. Salinity-induced physiological and molecular changes in barley and wheat. *Procedia Environ. Sci.* **2015**, *175*, 2950–2960. [CrossRef]
20. Ma, X.Y.; Jia, F.X.; Zhao, Y.L.; Zhao, J.C. Reference genes screening for quantitative real-time PCR in barley under drought and salt stress. *Mol. Plant Breed.* **2016**, *14*, 3093–3101.

21. Tang, X.; Zhang, N.; Si, H.; Calderón-Urrea, A. Selection and validation of reference genes for RT-QPCR analysis in potato under abiotic stress. *Plant Methods* **2017**, *13*, 85. [CrossRef] [PubMed]
22. Wang, H.L.; Chen, J.H.; Tian, Q.Q.; Wang, S.; Xia, X.L.; Yin, W.L. Identification and validation of reference genes for *Populus euphratica* gene expression analysis during abiotic stresses by quantitative real-time PCR. *Physiol. Plant.* **2014**, *152*, 529–545. [CrossRef] [PubMed]
23. Ri, X.; Yang, J.; Zhao, L.Q.; Qing, H.; Latanzhula, A.; Yao, Z.Y.; Zhu, L.; Wu, Y.H.; Tian, J.B.; Cao, X.P. Establishment, development, and decline of *Salix psammophila* communities: Changes in soil conditions and floristic composition in dune slacks. *Glob. Ecol. Conserv.* **2020**, *22*, e00967. [CrossRef]
24. Lu, D.Y.; Zhang, G.S.; Zhang, L.; Hao, L.; Huang, H.G. Progress in the research of *Salix psammophila*. *Mol. Plant Breed.* **2020**, *18*, 3427–3432.
25. Hao, L.H.; Zhang, L.Z.; Zhang, G.Z.; Wang, Y.W.; Han, S.H.; Bai, Y.B. Genetic diversity and population genetic structure of *Salix psammophila*. *Acta Bot. Boreali-Occident. Sin.* **2017**, *37*, 1507–1516.
26. Zhao, K.; He, R.; Zhang, G.; Qin, F.; Yue, Y.; Li, L.; Dong, X. Screening and expression characteristics of plant type regulatory genes in *Salix psammophila*. *Forests* **2024**, *15*, 103. [CrossRef]
27. Hao, L.; Zhang, G.S.; Mu, X.Y.; Han, S.L.; Wang, Y.; Ning, R.X.; Bai, Y.R.; Zhang, L. Phenotypic diversity of *Salix psammophila* populations in germplasm resources. *Acta Bot. Boreali-Occident. Sin.* **2017**, *37*, 1012–1021.
28. Sui, J.K.; Rao, G.D.; Zhang, J.G. Cloning and sequence analysis of *β-Tubulin Gene* families in willows. *Acta Bot. Boreali-Occident. Sin.* **2016**, *36*, 0902–0909.
29. Kim, D.; Ben, L.; Steven, L.S. HISAT: A fast spliced aligner with low memory requirements. *Nat. Methods* **2015**, *12*, 357–360. [CrossRef]
30. Trapnell, C.; Williams, B.A.; Pertea, G.; Mortazavi, A.; Kwan, G.; van Baren, M.J.; Salzberg, S.L.; Wold, B.J.; Pachter, L. Transcript assembly and quantification by RNA-seq reveals unannotated transcripts and isoform switching during cell differentiation. *Nat. Biotechnol.* **2010**, *28*, 511–515. [CrossRef]
31. Pertea, M.; Pertea, G.M.; Antonescu, C.M.; Chang, T.C.; Mendell, J.T.; Salzberg, S.L. StringTie enables improved reconstruction of a transcriptome from RNA-seq reads. *Nat. Biotechnol.* **2015**, *33*, 290–295. [CrossRef] [PubMed]
32. Tamura, K.; Stecher, G.; Peterson, D.; Filipski, A.; Kumar, S. MEGA6: Molecular Evolutionary Genetics Analysis Version 6.0. *Mol. Biol. Evol.* **2013**, *30*, 2725–2729. [CrossRef]
33. Jia, H.; Li, J.; Zhang, J.; Sun, P.; Lu, M.; Hu, J. The *Salix psammophila SpRLCK1* involved in drought and salt tolerance. *Plant Physiol. Biochem.* **2019**, *144*, 222–233. [CrossRef] [PubMed]
34. Zhu, J.K. Abiotic Stress Signaling and Responses in Plants. *Cell* **2016**, *167*, 313–324. [CrossRef] [PubMed]
35. Wang, L.; Sadeghnezhad, E.; Nick, P. Upstream of gene expression: What is the role of microtubules in cold signalling? *J. Exp. Bot.* **2020**, *71*, 36–48. [CrossRef] [PubMed]
36. Lloyd, C.; Hussey, P. Microtubule-associated proteins in plants—Why we need a map. *Nat. Rev. Mol. Cell Biol.* **2001**, *2*, 40–47. [CrossRef] [PubMed]
37. Zhu, J.; Lee, B.H.; Dellinger, M.; Cui, X.; Zhang, C.; Wu, S.; Nothnagel, E.A.; Zhu, J.K. A cellulose synthase-like protein is required for osmotic stress tolerance in *Arabidopsis*. *Plant J.* **2010**, *63*, 128–140. [CrossRef]
38. Zhu, J.K. Salt and drought stress signal transduction in plants. *Annu. Rev. Plant Biol.* **2002**, *53*, 247–273. [CrossRef]
39. Quarrie, S.A. Genotypic differences in leaf water potential, abscisic acid and proline concentrations in spring wheat during drought stress. *Ann. Bot.* **1980**, *46*, 383–394. [CrossRef]
40. Yang, H.; Zhang, L.; Li, A.; Hao, P.; Zhang, G.; Wei, D.; Fan, L.; Zhang, X.; Hu, J. Heterologous expression of *SpsLAZY1a* in *Populus* enhanced the sensitiveness of plant architecture. *Ind. Crop. Prod.* **2023**, *197*, 116572. [CrossRef]
41. Thomashow, M.F. Molecular basis of plant cold acclimation: Insights gained from studying the CBF cold response pathway. *Plant Physiol.* **2010**, *154*, 571–577. [CrossRef] [PubMed]